ISSN 1063-7745, Crystallography Reports, 2025, Vol. 70, No. 6, pp. 983–988. © Pleiades Publishing, Inc., 2025.

PHYSICAL PROPERTIES OF CRYSTALS

Computer Simulation of Fluorine Mobility in Solid Solutions with Fluorite Structure, $Pb_{0.8}M_{0.2}F_2$ and $Pb_{0.75}M_{0.2}K_{0.05}F_{1.95}$ (M = Ca, Ba)

Q. Ji[a], A. V. Petrov[a,*], A. K. Ivanov-Schitz[b], and I. V. Murin[a]

[a] *Institute of Chemistry, St. Petersburg State University, St. Petersburg, Russia*

[b] *Shubnikov Institute of Crystallography of the Kurchatov Complex of Crystallography and Photonics of the National Research Centre "Kurchatov Institute," Moscow, 119333 Russia*

**e-mail: a.petrov@spbu.ru*

Received April 2, 2025; revised April 25, 2025; accepted April 25, 2025

Abstract—The fluorine ion mobility in $Pb_{0.8}M_{0.2}F_2$ and $Pb_{0.75}M_{0.2}K_{0.05}F_{1.95}$ (M = Ca, Ba) solid solutions with fluorite structure under normal conditions was calculated using classical molecular dynamics. It was shown that isovalent substitution of lead atoms by calcium atoms in a lead fluoride crystal increases the mobility of fluorine ions, while a similar substitution by barium atoms decreases it. Heterovalent substitution Pb → K naturally increases the fluorine ion mobility in the $Pb_{0.75}Ca_{0.2}K_{0.05}F_{1.95}$ and $Pb_{0.75}Ba_{0.2}K_{0.05}F_{1.95}$ solid solutions.

DOI: 10.1134/S1063774525600577

INTRODUCTION

Fluorine-conducting solid solutions based on lead fluoride (obtained, in particular, by mechanochemical synthesis [1, 2]) are promising materials with a superhigh fluorine ion conductivity, which can be used in various electrochemical devices, including fluorine-ion batteries [3–6]. It is known that lead(II) fluoride may crystallize in two different modifications at different temperatures and pressures: orthorhombic (cotunnite structure) and cubic (fluorite structure). The fluorite structure determines the high mobility of anions, for example, in alkaline-earth fluorides, lead(II) fluoride, as well as zirconia and ceria (ZrO_2, CeO_2). The problem of stabilizing the fluorite structure under normal conditions is generally solved by isovalent or heterovalent doping of similar crystals. At the same time, doping of lead fluoride with heterovalent or homovalent fluorides may increase the ionic conductivity of the resulting materials to 10^{-3} S/cm at room temperature [7–11]. Doping of PbF_2 fluoride with alkaline-earth fluorides (CaF_2, SrF_2, BaF_2) forms a fluorite structure of solid solutions under normal conditions, and heterovalent doping increases the fluorine ion mobility [1, 12, 13]. Among such systems, the $Pb_{0.95}K_{0.05}F_{1.95}$ solid solution with the fluorite structure has the highest ionic conductivity ($\sigma = 3.55 \times 10^{-3}$ S/cm) at 300 K; at the same time, it is not stable enough at this temperature and gradually transforms into the cotunnite structure with a lower ionic conductivity [14]. The large amount of experimental studies of the materials based on lead fluoride stimulates further research into the nature of new compounds at the atomic and molecular levels in order to gain a detailed understanding of the mechanisms of ion transport in these materials.

The molecular dynamics (MD) method is efficiently used [15–18] to carry out computer simulation of multiparticle systems. Having analyzed the change in the particle coordinates and velocities in time in a modeled system, one can study in detail the dynamic processes and structural features of the modeled object. In this simulation, it is important to choose appropriate interatomic interactions for comparing with experimental physical and chemical data and predicting specific properties.

The MD simulation of the ion mobility in β-PbF_2 lead(II) fluoride shows [19–26] that the fluoride sublattice disordering facilitates the high mobility of fluorine ions, while the lead sublattice remains relatively stable [20, 21]. For lead fluoride doped with strontium and potassium fluorides, detailed information about the motion of fluorine ions could be obtained at the atomic level; it turned out to be in full agreement with the experimental data [19, 26].

In this study, the processes of ion transport and structural properties of solid solutions in the $Pb_{0.8}M_{0.2}F_2$ and $Pb_{0.75}M_{0.2}K_{0.05}F_{1.95}$ systems, where M = Ca, Ba, were studied using the MD method.

Table 1. Numbers of atoms in modeled cells

Modeled system	F	Pb	*M*	K	Number of atoms
β-PbF_2	1728	864	0	0	2592
$Pb_{0.8}M_{0.2}F_2$ (*M* = Ca, Ba)	1728	702	162	0	2592
$Pb_{0.75}M_{0.2}K_{0.05}F_{1.95}$ (*M* = Ca, Ba)	1674	648	162	54	2538

EXPERIMENTAL

The computation of the fluorine-ion mobility in the $Pb_{0.8}M_{0.2}F_2$ and $Pb_{0.75}M_{0.2}K_{0.05}F_{1.95}$ (*M* = Ca, Ba) solid solutions was performed using the Materials Studio software package and the GULP classical molecular dynamics module. The calculation parameters were as follows: *NVT* ensemble, temperature range 300–1000 K, simulation time 100 ps, integration step 1 fs.

At the first stage, a computational cell of the β-PbF_2 crystal with a cubic fluorite structure (sp. gr. $Fm\bar{3}m$) was constructed, with a size of 6 × 6 × 6 unit cells having periodic boundary conditions, and a cube side length of 3.56 nm. The computational cell sizes were chosen to be optimal, taking into account the available computer resources: further increase in the cell barely affected the calculation results, whereas the calculation time disproportionately increased. Then the lead atoms were randomly replaced with Ca or Ba atoms and with K atoms, according to the stoichiometry of the studied solid solutions; the numbers of atoms in the modeled systems are listed in Table 1.

A very important role in modeling the force field of ion crystals is played by atomic charges, which were calculated using the density functional theory method, implemented in the DMol^3 module of the Materials Studio software package (with the Perdew–Burke–Ernzerhof (PBE) functional (the generalized gradient approximation (GGA) functional), the Dynamic Nuclear Polarization (DNP) atomic basis, version 4.4, charge estimation according to the Mulliken scheme); the charge values were found to be $q = -0.9|e|$ for F, $q = 1.8|e|$ for Pb, Ca, Ba, and $q = 0.9|e|$ for K (*e* is the electron charge). The short-range action was modeled using the Buckingham potential with the atomic parameters calibrated based on the equilibrium geometry of dopant fluoride crystals.

The mobility of atoms was determined using their mean square displacements (MSD):

$$\mathrm{MSD}(t) = \frac{1}{N}\sum_{i=1}^{N}\left|\mathbf{r}_i(t_0 + \Delta t) - \mathbf{r}_i(t_0)\right|^2,$$

where *N* is the number of particles in the system, $\mathbf{r}_i(t_0)$ is the position vector of a particle *i* at the instant t_0, and $\mathbf{r}_i(t_0 + \Delta t)$ is the position vector of the particle *i* after a time step Δt.

The ion diffusion coefficients *D* were calculated from the Einstein relation:

$$D = \frac{1}{6}\lim_{t\to\infty}\frac{d}{dt}\mathrm{MSD}(t).$$

The structure of the local environment of ions in the modeled cell was studied using the radial distribution function (RDF):

$$g_{ab}(r) = \frac{\rho_{ab}(r)}{\rho},$$

where $\rho_{ab}(r)$ is the density of *a*-type particles in a spherical layer at a distance *r* from the *b*-type reference particle, and ρ is the density of *a* particles in the system.

RESULTS AND DISCUSSION

Structural characteristics. Figure 1 shows as an example the RDF of the $Pb_{0.8}Ca_{0.2}F_2$ solid solution for the anionic and cationic subsystems. It can be seen that all simulated phases form a fluorite-type lattice at 300 K, which is evidenced by the positions of the maxima for the first and second coordination spheres. With increasing temperature, the curve *g*(*r*) does not change qualitatively, but the fluorine-ion subsystem becomes disordered, which manifests itself in smoothing out and disappearance of the far-field peaks, while for the cation subsystems this effect is less pronounced.

Transport properties. Figure 2 shows the results of calculating the MSDs of F and Pb ions in crystals of the $Pb_{0.8}M_{0.2}F_2$ and $Pb_{0.75}M_{0.2}K_{0.05}F_{1.95}$ (*M* = Ca, Ba) solid solutions at temperatures of 600 and 1000 K.

It can be seen in Fig. 2 that the mobility of cations is very low: their diffusion coefficient does not exceed 10^{-10} cm^2/s up to 1000 K. In solid solutions where lead atoms are replaced with calcium atoms, the MSDs (and, therefore, mobility) of fluoride ions increase significantly as compared to pure β-PbF_2, whereas the mobility of fluorine ions decreases when lead atoms are replaced with barium atoms. Doping $Pb_{0.8}M_{0.2}F_2$ (*M* = Ca, Ba) solid solutions with a heterovalent substituent, potassium, increases the mobility of fluorine atoms, which confirms the trend of change in the transport properties of heterovalent solid solutions, being consistent with the experimental data [27].

Table 2 contains the values of the fluorine diffusion coefficients in β-PbF_2 and $Pb_{0.8}M_{0.2}F_2$, $Pb_{0.75}M_{0.2}K_{0.05}F_{1.95}$ (*M* = Ca, Ba) solid solutions at different temperatures, which were calculated using Eq. (2).

The diffusion activation energies E_a were found from the temperature dependences of D_F in the high-

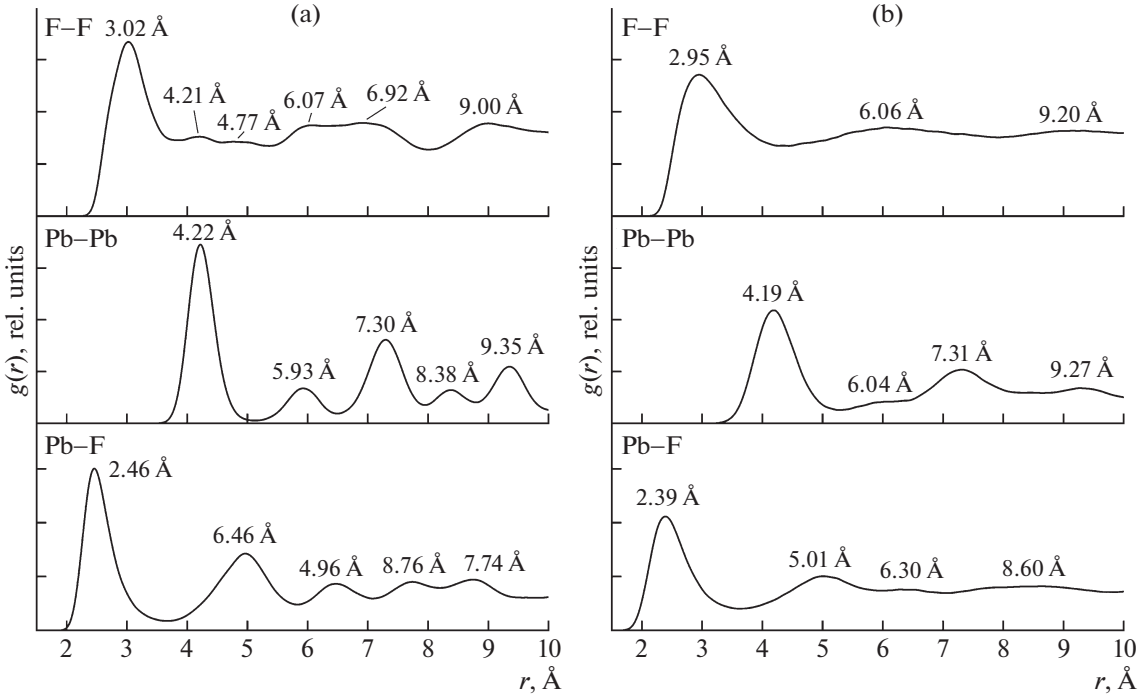

Fig. 1. Radial distribution functions for the $Pb_{0.8}Ca_{0.2}F_2$ system at (a) 300 and (b) 1000 K.

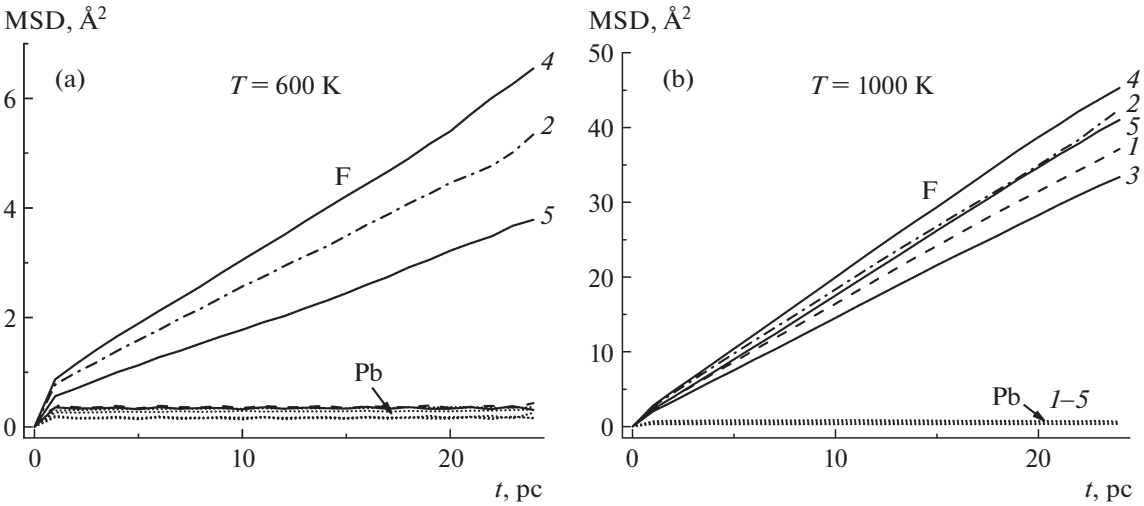

Fig. 2. RMS displacements of F^- and Pb ions in crystals of $Pb_{0.8}M_{0.2}F_2$ and $Pb_{0.75}M_{0.2}K_{0.05}F_{1.95}$ (M = Ca, Ba) solid solutions at temperatures of (a) 600 and (b) 1000 K: (*1*) β-PbF_2, (*2*) $Pb_{0.8}Ca_{0.2}F_2$, (*3*) $Pb_{0.8}Ba_{0.2}F_2$, (*4*) $Pb_{0.75}Ca_{0.2}K_{0.05}F_{1.95}$, and (*5*) $Pb_{0.75}Ba_{0.2}K_{0.05}F_{1.95}$.

temperature region (Fig. 3), according to the Arrhenius equation:

$$D_F = D_0 \exp\left(\frac{-E_a}{kT}\right),$$

where D_0 is the pre-exponential factor.

The increase in the diffusion activation energy in the studied solid solutions is qualitatively consistent (except for the $Pb_{0.8}Ba_{0.2}F_2$ composition) with direct experimental data on measuring the conductivity [27] (Table 3).

To explain the changes in the mobility of fluorine atoms at homo- and heterovalent doping of lead fluoride, we will consider in more detail the first peaks of the RDF functions presented in Fig. 4.

Table 2. Diffusion coefficients of fluorine atoms in β-PbF_2 and $Pb_{0.8}M_{0.2}F_2$, $Pb_{0.75}M_{0.2}K_{0.05}F_{1.95}$ (M = Ca, Ba) solid solutions at 300–1000 K, arranged in order of increasing diffusion

Calculation temperature, K	System	D_F, cm^2/s	Calculation temperature, K	D_F, cm^2/s
300	$Pb_{0.75}Ba_{0.2}K_{0.05}F_{1.95}$	4.13×10^{-7}	600	2.38×10^{-6}
	$Pb_{0.8}Ca_{0.2}F_2$	5.96×10^{-7}		3.30×10^{-6}
	$Pb_{0.75}Ca_{0.2}K_{0.05}F_{1.95}$	7.54×10^{-7}		4.11×10^{-6}
800	β-PbF_2	8.43×10^{-7}	1000	2.55×10^{-5}
	$Pb_{0.8}Ba_{0.2}F_2$	8.89×10^{-7}		2.30×10^{-5}
	$Pb_{0.75}Ba_{0.2}K_{0.05}F_{1.95}$	5.61×10^{-6}		2.84×10^{-5}
	$Pb_{0.8}Ca_{0.2}F_2$	1.43×10^{-5}		2.85×10^{-5}
	$Pb_{0.75}Ca_{0.2}K_{0.05}F_{1.95}$	1.57×10^{-5}		3.13×10^{-5}

In the $Pb_{0.8}Ca_{0.2}F_2$ solid solution, the average interatomic distance between fluorine and calcium atoms (1.80 Å) is smaller than the distance between fluorine and lead atoms (2.39 Å), which creates a larger volume of free space after the displacement of fluorine atoms towards calcium atoms and thus increases the possibility of anion migration. This effect is not observed in the $Pb_{0.8}Ba_{0.2}F_2$ solid solution. In addition, due to their large size, barium atoms hinder the formation of "free" space, thus weakening the migration of fluorine atoms. When heterovalent potassium atoms are introduced into the $Pb_{0.8}Ca(Ba)_{0.2}F_2$ matrix, vacancies of fluorine atoms are formed in the $Pb_{0.75}Ca_{0.2}K_{0.05}F_{1.95}$ and $Pb_{0.75}Ba_{0.2}K_{0.05}F_{1.95}$ solid solutions; they serve local compensators for the missing charge in the cation motif, increasing the mobility of fluorine atoms. Thus, the experimentally observed changes in the ionic mobility of fluorine atoms in the studied solid solutions are described well at the atomic level using the MD method; correspondingly, they may have predictive importance for the synthesis of new solid electrolytes with preferential conduction via fluorine ions,

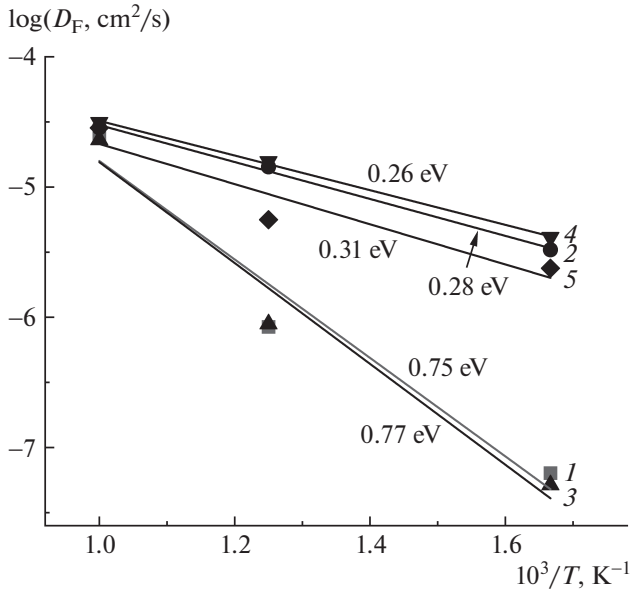

Fig. 3. Temperature dependences of the fluorine diffusion coefficient (D_F) for (*1*) β-PbF_2, (*2*) $Pb_{0.8}Ca_{0.2}F_2$, (*3*) $Pb_{0.8}Ba_{0.2}F_2$, (*4*) $Pb_{0.75}Ca_{0.2}K_{0.05}F_{1.95}$, and (*5*) $Pb_{0.75}Ba_{0.2}K_{0.05}F_{1.95}$. The numbers at the curves indicate the diffusion activation energies.

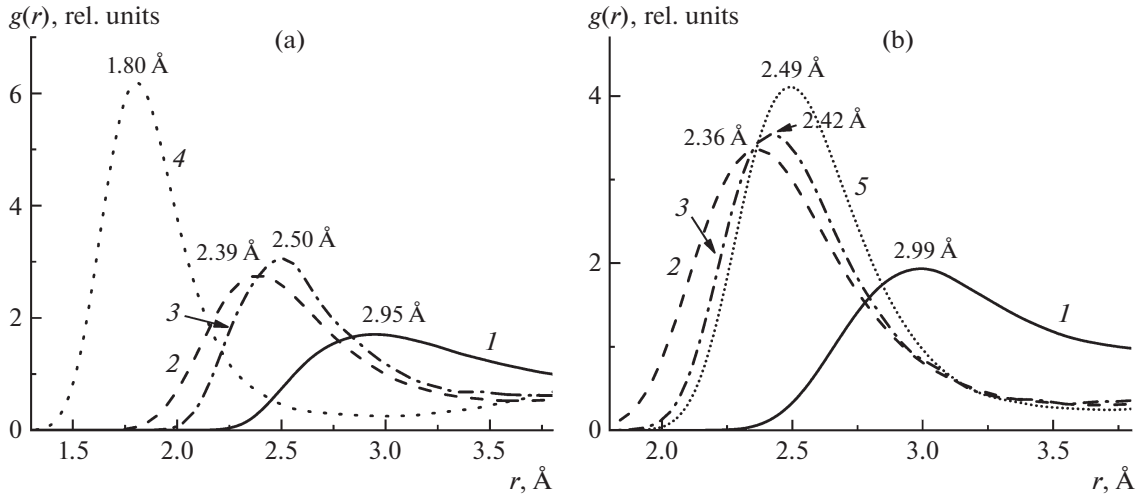

Fig. 4. Radial distribution functions between fluorine and metal atoms in the (a) $Pb_{0.75}Ca_{0.2}K_{0.05}F_{1.95}$ and (b) $Pb_{0.75}Ba_{0.2}K_{0.05}F_{1.95}$ solid solutions at 1000 K: pairs (*1*) F–F, (*2*) Pb–F, (*3*) K–F, (*4*) Ca–F, and (*5*) Ba–F.

based on lead fluoride with different homo- and heterovalent dopants.

CONCLUSIONS

The dynamic and structural properties of the $Pb_{0.8}Ca_{0.2}F_2$ and $Pb_{0.8}Ba_{0.2}F_2$ solid solutions with fluorite structure, based on lead fluoride, were calculated using the MD method. It was shown that the effect of isovalent doping with Ca and Ba atoms preserves the fluorite structure; at the same time, the introduction of Ca increases the fluorine ion mobility, while the introduction of Ba decreases it. The heterovalent replacement of lead with potaccium atoms naturally increases the fluorine-ion mobility in the $Pb_{0.75}Ca_{0.2}K_{0.05}F_{1.95}$ and $Pb_{0.75}Ba_{0.2}K_{0.05}F_{1.95}$ solid solutions due to the additional vacancy disordering of the fluorine sublattice.

Table 3. Diffusion and conductivity activation energies for the studied systems

Crystal	Diffusion activation energy (MD-calculation), eV	Conductivity activation energy (experiment [27]), eV
$Pb_{0.75}Ca_{0.2}K_{0.05}F_{1.95}$	0.26	0.20 ± 0.01
$Pb_{0.8}Ca_{0.2}F_2$	0.28	0.30 ± 0.01
$Pb_{0.75}Ba_{0.2}K_{0.05}F_{1.95}$	0.31	0.25 ± 0.01
β-PbF_2	0.75	0.57 ± 0.02
$Pb_{0.8}Ba_{0.2}F_2$	0.77	0.44 ± 0.01

ACKNOWLEDGMENTS

The study was performed using the computing resources of the Resource Center "Computing Center of St. Petersburg State University."

FUNDING

This work was carried out within an initiative project (no. 116881298, 2024) of St. Petersburg State University and within the State assignment for the National Research Centre "Kurchatov Institute."

CONFLICT OF INTEREST

The authors of this work declare that they have no conflicts of interest.

REFERENCES

1. Q. Ji, N. A. Melnikova, O. V. Glumov, et al., Ceram. Int. **49**, 16901 (2023). https://doi.org/10.1016/j.ceramint.2023.02.051
2. L. N. Patro, J. Solid State Electrochem. **24**, 2219 (2020). https://doi.org/10.1007/s10008-020-04769-x
3. S. V. Gopinadh, P. V. R. L. Phanendra, B. John, et al., Sustain. Mater. Technol. **32**, e00436 (2022). https://doi.org/10.1016/j.susmat.2022.e00436
4. M. A. Nowroozi, I. Mohammad, P. Molaiyan, et al., J. Mater. Chem. A **9**, 5980 (2021). https://doi.org/10.1039/D0TA11656D
5. T. Liu, N. Peng, X. Zhang, et al., Energy Storage Mater. **42**, 42 (2021). https://doi.org/10.1016/j.ensm.2021.07.011
6. M. Anji Reddy and M. Fichtner, J. Mater. Chem. **21**, 17059 (2011). https://doi.org/10.1039/c1jm13535j

7. I. V. Murin, Izv. SO AN SSSR, Ser. Khim., No. 1, **53** (1984).
8. W. D. Basler, I. V. Murin, and S. V. Chernov, Z. Naturforsch. A **36**, 519 (1981).
9. I. I. Buchinskaya and P. P. Fedorov, Russ. Chem. Rev. **73**, 371 (2004). https://doi.org/10.1070/RC2004v073n04ABEH000811
10. V. Y. Kavun, E. B. Merkulov, A. B. Slobodyuk, et al., J. Struct. Chem. **59**, 1572 (2018). https://doi.org/10.1134/S0022476618070089
11. V. Y. Kavun, A. B. Slobodyuk, S. L. Sinebryukhov, et al., Russ. J. Electrochem. **43**, 611 (2007). https://doi.org/10.1134/S1023193507060018
12. N. A. Melnikova, Q. Ji, B. Fei, et al., Russ. J. Gen. Chem. **94**, S28 (2024). https://doi.org/10.1134/S1070363224140044
13. A. Düvel, Dalton Trans. **48**, 859 (2019). https://doi.org/10.1039/C8DT03759K
14. A. K. Ivanov-Schitz and I. V. Murin, *Ionics of Solid State,* **Vol. 2** (S.-Peterb. Gos. Univ., St. Petersburg, 2010) [in Russian].
15. A. V. Petrov, Q. Ji, and I. V. Murin, Crystallogr. Rep. **69**, 220 (2024). https://doi.org/10.1134/S1063774524600145
16. I. Y. Gotlib, E. M. Piotrovskaya, and I. V. Murin, Comput. Mater. Sci. **36**, 73 (2006). https://doi.org/10.1016/j.commatsci.2004.12.078
17. T. T. Netshisaulu, A. V. Chadwick, P. E. Ngoepe, et al., J. Phys. Condens. Matter **17**, 6575 (2005). https://doi.org/10.1088/0953-8984/17/41/026
18. M. J. Castiglione and P. A. Madden, J. Phys. Condens. Matter **13**, 9963 (2001). https://doi.org/10.1088/0953-8984/13/44/311
19. A. V. Petrov, Q. Ji, and I. V. Murin, Russ. J. Gen. Chem. **92**, 2877 (2022). https://doi.org/10.1134/S1070363222120404
20. J. D. López, J. E. Diosa, and H. Correa, Ionics (Kiel) **25**, 5383 (2019). https://doi.org/10.1007/s11581-019-03073-7
21. A. B. Walker, M. Dixon, and M. J. Gillan, Solid State Ionics **5**, 601 (1981). https://doi.org/10.1016/0167-2738(81)90326-X
22. A. V. Petrov, M. S. Salamatov, A. K. Ivanov-Schitz, et al., Crystallogr. Rep. **64**, 932 (2019). https://doi.org/10.1134/S106377451905016X
23. J. D. López, J. E. Diosa, G. García, et al., Heliyon **8**, e09026 (2022). https://doi.org/10.1016/j.heliyon.2022.e09026
24. Y. Chergui, N. Nehaoua, B. Telghemti, et al., Eur. Phys. J. Appl. Phys. **51**, 20502 (2010). https://doi.org/10.1051/epjap/2010096
25. M. J. Castiglione, M. Wilson, P. A. Madden, et al., J. Phys. Condens. Matter **13**, 51 (2001). https://doi.org/10.1088/0953-8984/13/1/306
26. S. Watanabe, H. Matsuura, H. Akatsuka, et al., J. Nucl. Mater. **344**, 104 (2005). https://doi.org/10.1016/j.jnucmat.2005.04.025
27. Ts. Tszi, N. A. Mel'nikova, O. V. Glumov, et al., *Proc. All-Russia Scientific and Practical Conference "Fluoride Materials and Technologies," Moscow, April 15–19, 2024,* p. 119.

Translated by Yu. Sin'kov